

# Organoplatinum Complexes of the N,N-Diisopropyl-diazabutadiene Ligand: A Structural and Spectroscopic Study

Axel Klein<sup>\*a</sup>, Thilo Schurr<sup>a</sup>, and Stanislav Zális<sup>b</sup>

<sup>a</sup> Köln, Institut für Anorganische Chemie der Universität zu Köln

<sup>b</sup> Prague, J. Heyrovský Institute of Physical Chemistry, Academy of Sciences of the Czech Republic

Received March 4th, 2005.

*Professor Herbert W. Roesky zum 70. Geburtstag gewidmet*

**Abstract.** Organoplatinum complexes [Pt(R)<sub>2</sub>(iPr-DAB)], [PtCl(R)(iPr-DAB)] or [PtCl<sub>2</sub>(iPr-DAB)] (R = methyl or 2,4,6-trimethylphenyl = mesityl, iPr-DAB = N,N'-diisopropyl-1,4-diazabutadiene) have been investigated by a combination of multiple spectroscopy (NMR, UV/VIS), single crystal XRD and quantum chemical calculations. Excellent agreement of calculated and experimental structural data from XRD or NMR provide a good basis for the quantum mechanical calculations. DFT calculations reveal the contributions of the DAB ligand and the co-ligands to the electronic ground state. Methyl acts more or less purely as a  $\sigma$ -donor,

Cl or mesityl provide strong contributions ( $\sigma$  or  $\pi$ ) to the highest occupied molecular orbital (HOMO) whereas the lowest unoccupied molecular orbital (LUMO) is mainly centred to the DAB ligand. The TD-DFT calculated electronic transitions were in excellent agreement with the experimental ones and allow reliable assignment of the absorption bands.

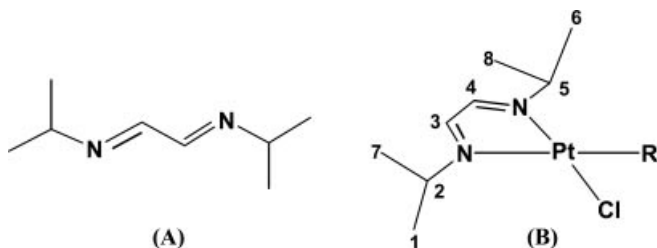
**Keywords:** Crystal structure; Platinum; Diimine ligands; NMR; Quantum chemical calculations

## Introduction

Platinum(II) complexes with  $\alpha$ -diimine ligands, their photo-physical properties and the resulting potential applications have been a subject of much interest in the last three decades [1–19]. Generally the low-energy electronic absorption bands are ascribed to metal-to-ligand charge transfer (MLCT) absorption bands. Correspondingly the lowest excited state is usually assumed to have MLCT character as well. These assignments agree with the pronounced solvatochromism and the extinction coefficients of the absorption bands. However in recent work we have explored the role of the co-ligands R in complexes of the type [Pt(R)<sub>2</sub>( $\alpha$ -diimine)] (R = alkyl, alkynyl or aryl) [16, 19]. By a combination of detailed spectroscopy (absorption, resonance Raman and emission) and DFT calculations it was shown that the R co-ligands contribute to the highest occupied molecular orbitals (HOMOs) and thus the electronic transitions and the excited states are better assigned to mixed MLCT/L'LCT (ligand-to-ligand charge transfer). This is most pronounced in cases where R possesses a  $\pi$ -system to interact with platinum or diimine  $\pi^*$ -orbitals.

In this study we want to extend this methodology to complexes with halogen (X) co-ligands since halogens are well known to contribute by  $\pi$  donation to excited states, which are then referred to XLCT instead of L'LCT. We have therefore synthesized and investigated a number of complexes using the most simple  $\alpha$ -diimine ligand N,N'-diisopropyl-1,4-diazabutadiene (Scheme 1). The DFT calculations on the halide containing complexes are underway to elucidate the electronic structure variation and consequent changes of physical properties due to the co-ligand variation.

Since in the above mentioned study [16, 19] the contribution of aryl or alkyl co-ligands was substantially different, we decided to examine two series of complexes: [Pt(R)<sub>2</sub>(iPr-DAB)]–[PtCl(R)(iPr-DAB)]–[PtCl<sub>2</sub>(iPr-DAB)] with R = methyl or mesityl (2,4,6-trimethylphenyl) since it has been shown that the overall donating power of methyl and mesityl is almost the same although the character of the contributions differs markedly [19].



**Scheme 1** Schematic representation of iPr-DAB = N,N'-diisopropyl-1,4-diazabutadiene in the non-coordinating free form (A) and in the square planar platinum(II) complex [PtCl(R)(iPr-DAB)] (B) with numbering of the C and corresponding H atoms.

\* Prof. Dr. A. Klein  
Universität zu Köln  
Institut für Anorganische Chemie  
Greinstraße 6  
D-50939 Köln  
e-mail: axel.klein@uni-koeln.de  
e-mail: zalis@jh-inst.cas.cz

Supporting information for this article is available on the WWW under <http://www.wiley-vch.de/home/zaac> or from the author

## Results and Discussion

### Preparation and analysis

The complexes [Pt(R)<sub>2</sub>(iPr-DAB)] (R = Me or Mes) have been synthesized as recently reported [16], [PtCl<sub>2</sub>(iPr-DAB)] was easily obtained from [PtCl<sub>2</sub>(dmsO)<sub>2</sub>] and the iPr-DAB ligand, the mixed compounds [PtCl(R)(iPr-DAB)] (R = Me or Mes) were prepared from the complexes [Pt(R)<sub>2</sub>(iPr-DAB)] using appropriate amounts of HCl generated in situ from acetyl chloride and methanol as similarly described by Clark and Manzer for the generation of [PtCl(Me)(COD)] from [Pt(Me)<sub>2</sub>(COD)] [20]. For details see the Experimental Part. Interestingly the reaction for R = Mes tolerates huge excesses of HCl (up to 5 times) yielding selectively [PtCl(Mes)(iPr-DAB)], for the preparation of [PtCl(Me)(iPr-DAB)] the exact 1:1 ratio is essential. Since also the "original" compound [Pt(Me)<sub>2</sub>(COD)] tolerates excesses of HCl, the *trans* directing power of the iPr-DAB ligand and not the bulkiness of the R co-ligands seems to be responsible for this effect.

### Crystal and molecular structures

The crystal and molecular structures of [PtCl(Me)(iPr-DAB)] was reported before (Vitagliano 1988) [21], all other compounds with the exception of [PtCl<sub>2</sub>(iPr-DAB)] were crystallized and successfully submitted to X-ray diffraction experiments.

The crystal structures of the complexes [Pt(Me)<sub>2</sub>(iPr-DAB)], [Pt(Mes)<sub>2</sub>(iPr-DAB)] and [PtCl(Mes)(iPr-DAB)] were all solved in the monoclinic P2<sub>1</sub>/n space group which contrasts to the orthorhombic Pca2<sub>1</sub> which was reported for [PtCl(Me)(iPr-DAB)] [21]. For [Pt(Me)<sub>2</sub>(iPr-DAB)] three independent molecules were found with almost identical molecular structure. In none of the structures we found significant intermolecular interactions other than van der Waals contacts. The crystallographic details are summarized in Table 1.

In all compounds the platinum atoms exhibit an almost perfect planar surrounding as can be seen e. g. from the dihedral angle NNPt/Cl<sub>n</sub>C<sub>m</sub>Pt. This is not the case for the reported [PtCl(Me)(iPr-DAB)] in which the chlorine atom deviates markedly, leading to a NNPt/Cl<sub>n</sub>C<sub>m</sub>Pt dihedral angle of 11.3° [21]. The overall structure of [PtCl(Me)(iPr-DAB)] seems to be very poor (if not incorrect) and we will not discuss any structural details from this structure. Furthermore we did not succeed to get a crystal structure for [PtCl<sub>2</sub>(iPr-DAB)]. We have therefore calculated all molecular structures using both Gaussian and ADF methods. The calculated data are in good agreement with the experimental ones (see Supporting Information) the results from ADF/BP calculations were slightly better in that respect. Table 2 lists combined essential experimental and calculated structural data of all compounds, Figure 1 shows selected molecular structures.

The bite angles N–Pt–N are almost identical for all complexes. For related platinum DAB complexes the values

range from 76 to 79° [22–24] indicating that the bite angle is a crucial (and thus more or less invariable) structural parameter. The Pt–N, Pt–C and Pt–Cl bond lengths are also in the expected range when compared to related structures. Within the series of complexes the experimentally observed or calculated distances follow nicely the trends expected from *trans* or *cis* influence [25, 26]: a strong ligand *trans* to a regarded bond will be lengthening the bond (*trans* influence) while a *cis* oriented strong ligand has an opposed effect (*cis* influence) albeit usually to a much smaller extent. E.g. the Pt–N distance decreases in the following series with *trans(cis)* positioned co-ligands Me(Cl) > Mes(Cl) > Mes(Mes) > Me(Me) > Cl(Cl). The series reveals a slightly superior *trans* influence of the Me co-ligand compared to Mes and the lengthening effect of the weak *cis*-oriented Cl co-ligand compared to the R co-ligands (*cis* influence). The Mes co-ligand is not oriented perfectly perpendicular to the coordination plane (Cl<sub>n</sub>R<sub>m</sub>PtNN). The dihedral angles were around 70° for (Mes)<sub>2</sub> and 81.2° for Cl(Mes). Very similar angles were found in numerous aryl platinum complexes with π-accepting ligands like diimines [19] pointing to an adoption of the angles to allow optimum electronic interaction of the Mes co-ligand with the platinum centre and the π-accepting ligand. We can therefore conclude that the Mes co-ligand is not only restricted to σ interaction but might exert some π contributions.

### NMR Spectroscopy and calculations

All complexes were studied by <sup>1</sup>H and <sup>13</sup>C NMR spectroscopy to probe for the impact of the R or Cl co-ligands. At the same time essential NMR parameters were calculated for the model complexes with the Me-DAB ligand. Table 3 summarizes essential experimental and ADF calculated <sup>1</sup>H or <sup>13</sup>C NMR data, full NMR data is deposited in the Supporting Information.

When comparing the H–Pt or C–Pt coupling constants of the iPr-DAB ligand which are relevant for discussing the *trans* or *cis* influence of the co-ligands we always find decreasing coupling constants along the series of *trans(cis)* positioned co-ligands Cl(Mes) > Cl(Me) > Cl(Cl) > Mes(Mes) > Me(Me). The series goes nicely along with an decreasing *trans* influence Mes > Me > Cl (strengthening the metal ligand coupling) superimposed with an increasing *cis* influence Cl < Me < Mes which also enhances the metal ligand coupling. The calculated values agree reasonably well for the <sup>1</sup>H data, only the Cl(Mes) and Cl(Me) are changed in sequence. For the calculated <sup>13</sup>C data the largest C–Pt coupling is obtained for the Cl(Cl) derivative. Generally the coupling constants are very sensitive to geometry but also to solvent effects which were not included here. Obviously this leads to an overestimation of the strengthening influence of the Cl co-ligand on the coupling constant. The series of co-ligand influence, although with a changed sequence for the Mes and Me, was also deduced from the crystal structures. However since the differences found in the structures between Mes and Me were small and in crystal structures packing forces and related

**Table 1** Crystal structure and refinement data for iPr-DAB platinum complexes <sup>a)</sup>

	(Me) <sub>2</sub>	(Mes) <sub>2</sub>	Cl(Mes)
Formula	C <sub>10</sub> H <sub>22</sub> N <sub>2</sub> Pt <sub>1</sub>	C <sub>26</sub> H <sub>38</sub> N <sub>2</sub> Pt <sub>1</sub>	C <sub>17</sub> H <sub>27</sub> Cl <sub>1</sub> N <sub>2</sub> Pt <sub>1</sub>
Formula weight	365.39	573.67	489.95
Space group	P2 <sub>1</sub> /n	P2 <sub>1</sub> /n	P2 <sub>1</sub> /n
unit cell	a / Å b / Å c / Å β / °	9.6570(19) 11.427(2) 15.765(3) 14.699(3)	9.0739(17) 13.249(3) 15.318(3) 102.483(15)
volume / Å <sup>3</sup> , Z	3890.6(13) 12	2542.9(9) 4	1798.0(6) 4
δ <sub>calc.</sub> / (mg·m <sup>-3</sup> )	1.871	1.498	1.810
absorption coefficient. / mm <sup>-1</sup>	10.785	5.531	7.949
F(000)	2088	1144	952
crystal size / mm	0.3 x 0.1 x 0.1	0.4 x 0.2 x 0.1	0.35 x 0.25 x 0.15
Colour	violet	violet	red
θ range / °	1.76 to 25.00	1.94 to 27.00	2.05 to 27.50
limiting indices	-1 < h < 11, -3 < k < 38, -15 < l < 14	-14 < h < 14, 0 < k < 20, 0 < l < 18	-8 < h < 11, -14 < k < 17, -19 < l < 19
reflect. collected	7278	5550	4327
independent (R <sub>int</sub> )	6848 (0.0796)	5550 (0.0678)	4081 (0.0485)
data/restr./param.	6848 / 1 / 370	5550 / 0 / 273	4081 / 0 / 197
gof on F <sup>2</sup>	1.143	1.074	1.022
final R <sub>I</sub>	0.0659	0.0695	0.0492
indices wR <sub>2</sub>	0.1296	0.1705	0.0859
R indices R <sub>J</sub>	0.1292	0.1069	0.1030
(all data) wR <sub>2</sub>	0.1557	0.1942	0.1008
largest diff. peak and hole / e Å <sup>-3</sup>	1.414 and -1.401	2.176 and -2.921	1.898 and -0.988

<sup>a)</sup> Measurements at 173(2) K, Radiation wavelength λ = 0.71073 Å; Refinement method: Full-matrix least-squares on F<sup>2</sup>; Absorption correction: empirical, psi-scans.

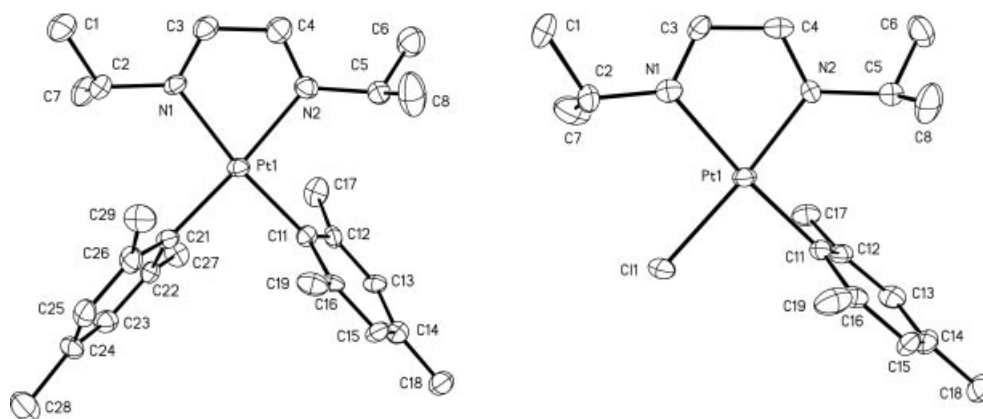


**Figure 1** View of [Pt(Mes)<sub>2</sub>(iPr-DAB)] (left) and [PtCl(Mes)(iPr-DAB)] from crystal structure determination (with numbering). The atoms are represented by 30 % thermal ellipsoids.

phenomena could be superimposed we feel a higher degree of reliance for the concluded series from NMR data. Furthermore it is interesting to note that although the two imine protons in the unsymmetrical complexes [PtCl(R)(iPr-DAB)] are clearly non-equivalent, their <sup>3</sup>J<sub>HH</sub> coupling is too small to be detected.

### UVVIS absorption spectroscopy and electronic states

The compounds under investigation vary in their colour from red (Cl<sub>2</sub>) to deep violet (Me<sub>2</sub>) in the solid as well as in solution. Figure 2 shows representative spectra, the long-wavelengths absorption maxima are listed in Table 4. All compounds exhibit strong negative solvatochromism (red

shift in unpolar solvents) which is a strong argument for a charge transfer transition being responsible for the colours. On first view all spectra consist of three main band systems, a broad structured band of medium intensity around 500 nm, a surprisingly invariant band at 360 nm of almost the same intensity and finally sharp bands, also almost invariant, at 238 nm. The first two are tentatively assigned to charge transfer transitions, the latter to π→π\*<sub>DAB</sub> transitions. From the data we can conclude complexes containing the Mes co-ligand show markedly lower lying electronic transitions than the corresponding Me derivatives and the long-wavelength absorption bands are more complex.

In order to assign the observed absorptions we have calculated the electronic ground states by DFT methods and

**Table 2** Selected structural data for iPr-DAB platinum complexes [PtCl<sub>n</sub>(R)<sub>m</sub>(iPr-DAB)]

distances / Å	(Me) <sub>2</sub> <sup>a)</sup>	(Mes) <sub>2</sub>	Cl(Me), calc <sup>b)</sup>	Cl(Mes)	Cl <sub>2</sub> , calc <sup>b)</sup>
Pt1–N1	2.034(19)	2.099(9)	2.126	2.113(7)	2.010
Pt1–N2	2.085(13)	2.110(10)	1.996	1.998(7)	2.010
Pt1–C11 (Cl2)	2.05(2)	2.022(11)	2.051	2.022(9) (C)	2.289
Pt1–C21 (Cl1)	2.049(16)	2.038(12)	2.283	2.286(2) (Cl)	2.289
C3–C4	1.46(3)	1.468(19)	1.429	1.438(13)	1.433
N1–C3	1.27(2)	1.274(16)	1.303	1.269(11)	1.314
N2–C4	1.30(2)	1.274(17)	1.318	1.301(11)	1.314
N1–C2	1.48(2)	1.489(15)	1.452	1.469(12)	1.459
N2–C5	1.47(2)	1.471(16)	1.451	1.490(12)	1.459
angles / °					
N1–Pt1–N2	78.9(6)	77.8(4)	78.0	78.4(3)	79.3
N2–Pt1–C11	96.8(8)	94.9(4)	98.0	96.5(3)	95.4
C11–Pt1–C21	88.1(9)	90.1(5)	87.4	88.3(3) (Cl)	89.9
N1–Pt1–C21	96.1(8)	97.3(4)	96.5	96.9(2) (Cl)	95.4
N1–Pt1–C11	175.6(8)	172.4(4)	176.0	174.4(3)	174.7
N2–Pt1–C21	175.0(8)	174.0(4)	174.5	175.2(2) (Cl)	174.7
torsion / dihedral angles / °					
N1–C3–C4–N2	2(3)	0.5(19)	0.0	2.7(13)	0.6
C2–N1–C3–C4	178.2(16)	175.4(11)	179.8	178.0(9)	179.7
C5–N2–C4–C3	177.0(16)	173.2(11)	179.8	177.3(8)	179.8
NNPt/Cl <sub>n</sub> C <sub>m</sub> Pt	1.1, 2.8, 2.9	4.1	0.1	2.5	1.3
Mes/coord-plane <sup>c)</sup>	–	70.2, 72.3	–	81.2	–

<sup>a)</sup> Values from molecule 1. <sup>b)</sup> ADF/BP calculated for the corresponding Me-DAB model complex. <sup>c)</sup> Coordination plane as defined by NNPtCl<sub>n</sub>C<sub>m</sub>.

**Table 3** Selected ADF/BP calculated and experimental <sup>1</sup>H and <sup>13</sup>C NMR data of iPr-DAB platinum complexes [PtCl<sub>n</sub>(R)<sub>m</sub>(iPr-DAB)]<sup>a)</sup>

	<sup>1</sup> H		<sup>13</sup> C				
	H3,4 exp.	H3,4 calc. <sup>b)</sup>	CH <sub>3</sub> exp.	C3,4 exp.	C3,4 calc. <sup>b)</sup>	PtC exp.	C2,5 exp.
Me <sub>2</sub>			PtCH <sub>3</sub>			PtC	
δ	8.99	7.39	1.47	158.1	146.7	–15.1	
JPt (Hz)	34.0	35.6	85.2	14.6	44.7	785	
Cl(Me)			PtCH <sub>3</sub>			PtCH <sub>3</sub>	
δ	8.54, 9.02	7.29, 7.38	1.49	160.5 158.1	149.5, 144.3	–13.0	
JPt (Hz)	36.3, 106.2	36.2, 112.4	78.5	6.9, 60.0	69.4, 84.8	706.7	
(Mes) <sub>2</sub>			oCH <sub>3</sub>			PtCl	
δ	8.96	7.40	2.33	157.5	146.2	135.6	55.9
JPt (Hz)	36.8	37.0	6.2	25.4	45.3	1174	39.2
Cl(Mes)			OCH <sub>3</sub>			PtCl	
δ	8.47, 8.98	7.28, 7.38	2.33	161.5, 159.8	150.3, 145.3	135.9	57.9, 60.3
JPt (Hz)	36.4, 108.6	34.5, 106.9	8.3	< 13, 68.8	69.8, 86.2	956.1	26.6, 75.9
Cl <sub>2</sub>							
δ	8.54	7.20	–	162.2	148.3		59.4
JPt (Hz)	98.5	90.4	–	n.d. <sup>c)</sup>	116.7		n.d. <sup>c)</sup>

<sup>a)</sup> All measured in CDCl<sub>3</sub>, numbering according to scheme 1. <sup>b)</sup> Calculated for Me-DAB model complexes. <sup>c)</sup> Not detectable due to very low solubility.

electronic transitions using TD-DFT for the two model complexes [PtCl(R)(Me-DAB)]. Here the G03/B3LYP method was used since it allows excellent incorporation of solvent effects (G03/B3LYP/CPCM) for the calculation of electronic transitions. Figure 3 visualizes the qualitative MO scheme calculated for the ground states of the two Cl(R) compounds, the full data (including [PtCl<sub>2</sub>(Me-DAB)]) can be found in the Supporting Information. Figure 3 reveals the different contributions of the Mes, Me and Cl co-ligands: The lowest unoccupied molecular orbital (LUMO) is in each case predominantly formed by the lowest DAB π\* orbital. If Cl is present, high lying occupied MO are found with very mixed d<sub>Pt</sub> + p<sub>Cl</sub> character. For the Cl(Me) and the Cl<sub>2</sub> derivative such orbitals form the highest occupied MO (HOMO). Complexes containing the Mes co-ligand exhibit additional levels which can be described as

pure π(Mes) or mixed d<sub>Pt</sub> + π<sub>Mes</sub> orbitals. Figure 4 shows some of the above discussed occupied orbitals of [PtCl(Mes)(Me-DAB)]. The electronic situation for the Me<sub>2</sub> derivative which has been reported recently [16] is characterized by a moderate to small contribution (12 %) of the Me sp<sup>3</sup> hybrid orbitals to the mainly metal (d<sub>Pt</sub>) centred HOMO, a contribution that is entirely missing in the Cl(Me) derivative. Although NMR and UV/Vis spectroscopy have revealed that the Me co-ligand is a very strong ligand, he provides virtually no other contribution than to (de)stabilise platinum orbitals as a strong σ donor.

The energies of the calculated electronic transitions for the two model complexes [PtCl(R)(Me-DAB)] (R = Mes or Me) agree quite well with the experimental data (Table 5 and Table 6). Only the calculated long-wavelength transition in [PtCl(Me)(iPr-DAB)] is markedly lower in energy

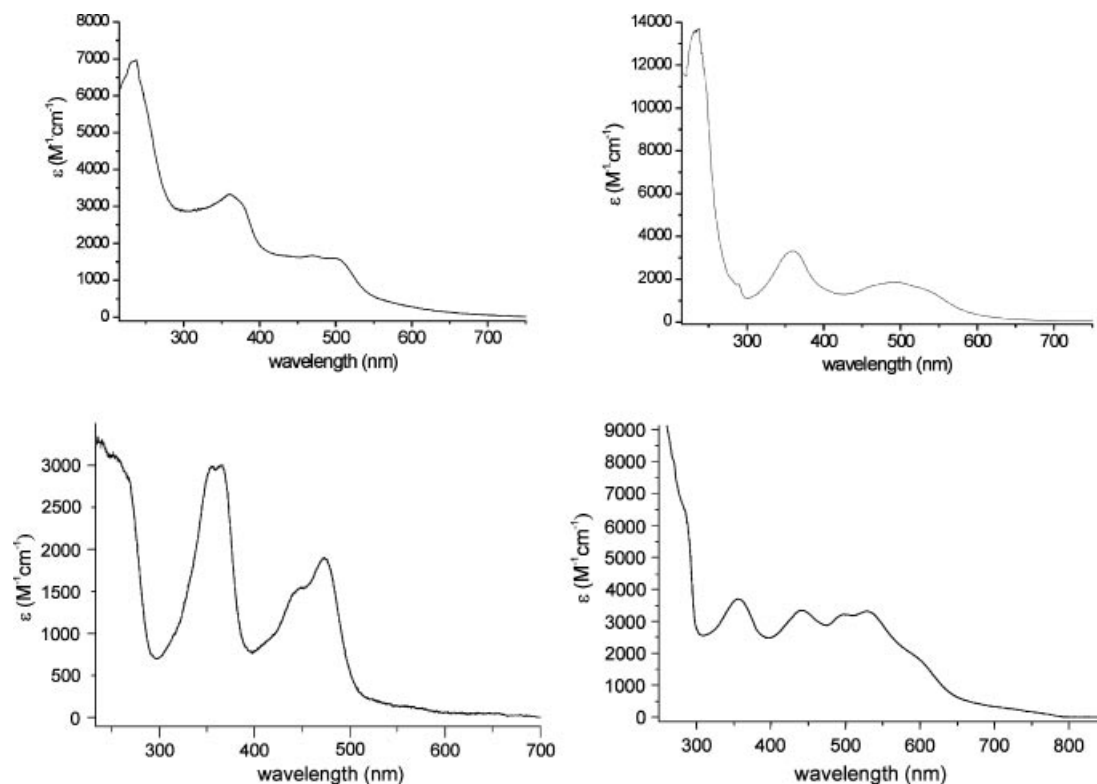


**Figure 2** Absorption spectra of [PtCl(Me)(iPr-DAB)] (top, left), [PtCl(Mes)(iPr-DAB)] (top, right) [PtCl<sub>2</sub>(iPr-DAB)] (bottom, left) and [Pt(Mes)<sub>2</sub>(iPr-DAB)] (bottom, right) all in CH<sub>2</sub>Cl<sub>2</sub> solution.

**Table 4** Observed electronic absorption maxima for complexes [PtCl<sub>n</sub>(R)<sub>n</sub>(iPr-DAB)]<sup>a)</sup>

compound	λ <sub>6</sub> (ε)	λ <sub>5</sub> (ε)	λ <sub>4</sub> (ε)	λ <sub>3</sub> (ε)	λ <sub>2</sub> (ε)	λ <sub>1</sub> (ε)
(Me) <sub>2</sub>	234 (17.0)	–	390 (3.3)	543 (2.5)	–	–
(Mes) <sub>2</sub>	237 (15.8)	281sh (6.5)	355 (3.6)	438 (3.3)	533 (3.3)	581sh (2.2)
Cl(Mes)	238 (13.5)	286 (1.8) <sup>b)</sup>	359 (3.4)	492 (1.9)	535sh (1.5)	598sh (0.4)
Cl(Me)	238sh (7.6)	265sh (4.2) <sup>c)</sup>	362 (3.3)	498 (1.5)	–	–
Cl <sub>2</sub>	238 (3.0)	258 (3.0)	364 (3.0)	471 (1.9)	–	–

<sup>a)</sup> Measured in CH<sub>2</sub>Cl<sub>2</sub>, absorption maxima in wavelength [in nm] the molar extinction coefficients ε are given in parentheses (in 1000 M<sup>-1</sup>cm<sup>-1</sup>). <sup>b)</sup> Further maximum at 276 nm (sh, ε = 2.1). <sup>c)</sup> Further maximum at 291 nm (sh, ε = 2.9).

than the experimentally found lowest band. The calculated oscillator strength agree only qualitatively with the observed intensities. However the overall agreement between calculated and experimental data presented here is far better compared to the previous TD-DFT calculations with solvent cage modelled by the polarizable continuum model (PCM) [27] for the complexes [Pt(R)<sub>2</sub>(Me-DAB)] and [Pt(R)<sub>2</sub>(iPr-DAB)] (R = methyl or aryl) [16]. In the G03/B3LYP/CPCM method applied in this work the CPCM is included in the TD-DFT formalism giving better agreement between calculated and experimental energies.

We can therefore assign the long-wavelength absorptions for [PtCl(Me)(iPr-DAB)] to two electronic transitions of mixed metal(d<sub>Pt</sub>)-to-ligand(π\*<sub>DAB</sub>) / chlorine-to-ligand charge transfer (MLCT/XLCT) character. The starting orbitals (HOMO to HOMO-3) are of mixed d<sub>Pt</sub> + p<sub>Cl</sub> character and the target orbital is the 13a'' LUMO (π\*<sub>DAB</sub>). The intense absorption around 360 nm is due to a transition

with mainly MLCT character. The intense band around 240 nm consists of two individual transitions with mainly π<sub>DAB</sub>→π\*<sub>DAB</sub> character. For the complex [PtCl(Mes)(iPr-DAB)] the three long-wavelength absorptions at 530 and 500 nm can be assigned to mixed MLCT/XLCT transitions and the band at 360 nm to a more or less pure MLCT transition as discussed above for the Cl(Me) derivative. The following band at 286 nm is markedly weaker than the previous charge transfer bands. Following our TD-DFT calculations this band can be assigned to a mixed transition (e<sup>1</sup>A) in which the target orbital has a high d<sub>Pt</sub> contribution. In a simplified way this corresponds to the ligand field transition (d<sub>xy</sub>→d<sub>x<sup>2</sup>-y<sup>2</sup></sub>) in a d<sup>8</sup> system. The same type of transition was also calculated for the Cl(Me) derivative (c<sup>1</sup>A'), however in the corresponding spectrum this band is not resolved but appears as a shoulder. The next calculated transition (267 nm) can be observed as a shoulder at 276 nm. The corresponding transition is again of mixed MLCT/

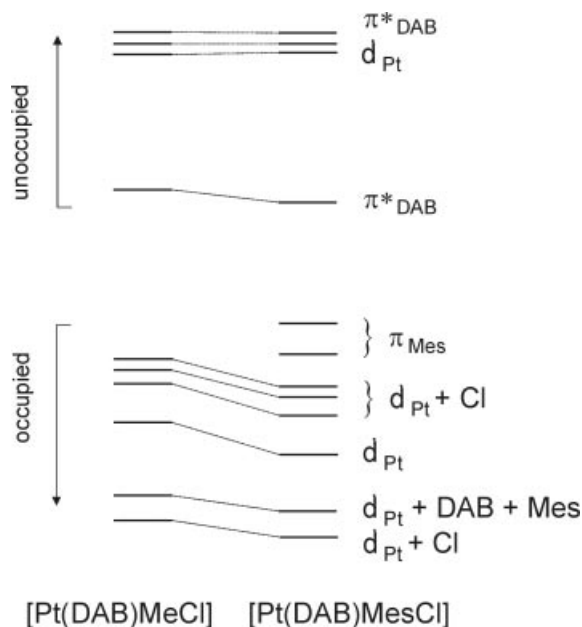


**Figure 3** Calculated electronic levels in [PtCl(Me)(Me-DAB)] (left) and [PtCl(Mes)(Me-DAB)] (right).

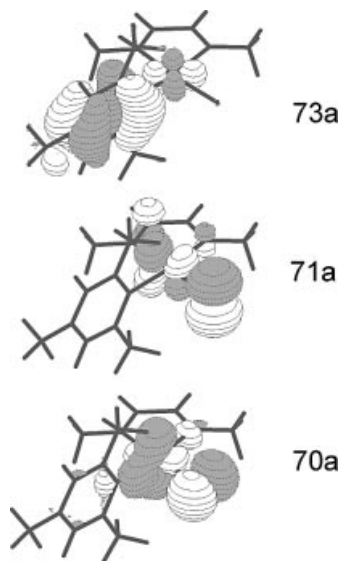


**Figure 4** The HOMO **73a** ( $\pi_{\text{Mes}}$ ), HOMO-2 **71a** and HOMO-3 **70a** ( $d_{\text{Pt}} + p_{\text{Cl}}$ ) orbitals of [PtCl(Mes)(Me-DAB)]

**Table 5** TD-DFT G03/B3LYP/CPCM ( $\text{CH}_2\text{Cl}_2$ ) singlet excitation energies (eV) for [PtCl(Me)(Me-DAB)] with oscillator strength larger than 0.001.

State	Main components (%)	Transition energy in eV (nm)	Osc. strength	Exper. trans. in nm	Ext. coeff. a)
$b^1A'$	83 ( $12a'' \rightarrow 13a''$ ); 16 ( $11a'' \rightarrow 13a''$ )	2.37 (522)	0.005	498	1.5
$a^1A''$	84 ( $28a' \rightarrow 13a''$ ); 15 ( $27a' \rightarrow 13a''$ )	2.38 (521)	0.002	498	1.5
$b^1A'$	75 ( $11a'' \rightarrow 13a''$ ); 14 ( $12a'' \rightarrow 13a''$ )	3.25 (382)	0.137	362	3.3
$d^1A'$	84 ( $28a' \rightarrow 29a'$ ); 10 ( $27a' \rightarrow 29a'$ )	4.41 (281)	0.010	291sh	2.9
$d^1A'$	71 ( $10a'' \rightarrow 13a''$ ); 13 ( $27a' \rightarrow 29a'$ )	4.63 (267)	0.025	265sh	4.2
$e^1A'$	71 ( $9a'' \rightarrow 13a''$ ); 13 ( $10a'' \rightarrow 13a''$ );	5.37 (230)	0.136	238sh	7.6

a) Extinction coefficient in  $1000 \text{ M}^{-1} \text{ cm}^{-1}$ .

XLCT character. The UV absorption at 238 nm can be assigned to a  $\pi_{\text{Mes}} \rightarrow \pi^*_{\text{DAB}}$  transition. Obviously the two systems [PtCl(R)(iPr-DAB)] differ markedly in the UV region: For the Cl(Me) derivative two individual  $\pi_{\text{DAB}} \rightarrow \pi^*_{\text{DAB}}$  transitions were calculated and in both cases the LUMO is the main target orbital. For the Cl(Mes) derivative the transition ( $g^1A$ ) has mainly  $\pi_{\text{Mes}} \rightarrow \pi^*_{\text{DAB}}$  character and the target orbital is mainly the LUMO+2. Our calculated data thus well explains the obvious differences in the experimental spectra – Cl(Me): two bands of medium strength vs. Cl(Mes): one very strong band.

## Experimental Part

### Synthesis

All preparations and manipulations were carried out under an inert atmosphere of argon or nitrogen. All complexes were prepared and examined under the protection from intense light. The dimethyl or dimesityl complexes [Pt(R)<sub>2</sub>(iPr-DAB)] (R = Me or Mes) were prepared as previously published for related complexes [16–18] from [Pt(CH<sub>3</sub>)<sub>2</sub>(COD)] (COD = 1,5-cyclooctadiene [20] or [Pt(Mes)<sub>2</sub>(dmsO)<sub>2</sub>] [28] and the iPr-DAB ligand and analyzed correctly. The halogeno complexes [PtCl(R)(iPr-DAB)] were generated by addition of an excess of HCl (from acetyl chloride and methanol) in toluene in the same way described by Clark and Manzer [20] for [PtCl(Me)(COD)]. [PtCl(Me)(iPr-DAB)] was obtained as deep red microcrystalline material in 95% yield. Anal. Calcd. for C<sub>9</sub>H<sub>19</sub>N<sub>2</sub>ClPt: C 28.02, H 4.96, N 7.26%. Found: C 28.05, H 4.99, N 7.22%.

<sup>1</sup>H NMR (CDCl<sub>3</sub>):  $\delta$ : 1.44 (d, 6 H, <sup>3</sup>J = 6.59 Hz, H1,7), 1.47 (d, 6 H, <sup>3</sup>J = 6.62 Hz, H6,8), 1.49 (s, 3 H, <sup>3</sup>J<sub>PtH</sub> = 78.5 Hz, PtCH<sub>3</sub>), 4.71 (septet, 1 H, H5), 4.81 (septet, 1 H, H2), 8.54 (s, 1 H, <sup>3</sup>J<sub>PtH</sub> = 36.3 Hz, H3), 9.02 (s, 1 H, <sup>3</sup>J<sub>PtH</sub> = 106.2 Hz, H4).

[PtCl(Mes)(iPr-DAB)] was obtained as red violet microcrystalline material in 97% yield. Anal. Calcd. for C<sub>17</sub>H<sub>27</sub>N<sub>2</sub>ClPt: C 41.67, H 5.55, N 5.72%. Found: C 41.69, H 5.59, N 5.77%.

<sup>1</sup>H NMR (CD<sub>2</sub>Cl<sub>2</sub>):  $\delta$ : 1.19 (d, 6 H, <sup>3</sup>J = 6.4 Hz, H1,7), 1.52 (d, 6 H, <sup>3</sup>J = 6.5 Hz, H6,8), 2.18 (s, 3 H, p-CH<sub>3</sub>), 2.33 (s, 6 H, <sup>4</sup>J = 6.4 Hz, o-CH<sub>3</sub>), 4.04 (septet, 1 H, H5), 4.79 (septet, 1 H, H2), 6.57 (s, 2 H, HMes), 8.47 (s, 1 H, <sup>3</sup>J = 36.4 Hz, H3), 8.98 (s, 1 H, <sup>3</sup>J<sub>PtH</sub> = 108.6 Hz, H4)

[PtCl<sub>2</sub>(iPr-DAB)]. [PtCl<sub>2</sub>(dmsO)<sub>2</sub>] (211 mg, 0.5 mmol) and iPr-DAB (73 mg, 0.52 mmol) were stirred together in 50 mL of CH<sub>2</sub>Cl<sub>2</sub> for 5 hours. After addition of 30 mL of *n*-heptane the volume is reduced to 50 mL during which a orange/red precipitate forms. The collected solid was washed with pentane and recrystallized from CH<sub>2</sub>Cl<sub>2</sub> to give a red microcrystalline material. Yield: 98%. Anal. Calcd. for C<sub>8</sub>H<sub>16</sub>N<sub>2</sub>Cl<sub>2</sub>Pt: C 23.65, H 3.97, N 6.90%. Found: C 23.69, H 3.99, N 6.90%.

**Table 6** TD-DFT G03/B3LYP/CPCM (CH<sub>2</sub>Cl<sub>2</sub>) singlet excitation energies(eV) for [PtCl(Mes)(Me-DAB)] with oscillator strength larger than 0.001.

State	Main components (%)	Transition energy (eV)	Osc. strength	Exper. trans. (eV)	Ext. coeff. a)
b <sup>1</sup> A	96 (71a→74a)	2.27 (546)	0.002	535sh	1.5
c <sup>1</sup> A	69 (70a→74a); 18 (68a→74a)	2.46 (503)	0.012	492	1.9
d <sup>1</sup> A	78 (68a→74a); 17 (70a→74a)	3.30 (376)	0.145	359	3.4
e <sup>1</sup> A	78 (71a→75a); 14 (69a→75a)	4.35 (285)	0.023	286	1.8
f <sup>1</sup> A	78 (66a→74a)	4.64 (267)	0.049	276sh	2.1
g <sup>1</sup> A	78 (73a→77a)	5.49 (226)	0.232	238	13.5

a) Extinction coefficient in 1000 M<sup>-1</sup>·cm<sup>-1</sup>.

<sup>1</sup>H NMR (CD<sub>2</sub>Cl<sub>2</sub>): δ: 1.50 (d, 12 H, <sup>3</sup>J = 6.78 Hz, H1,6,7,8), 5.14 (septet, 2 H, H2,5), 8.51 (s, 2 H, <sup>3</sup>J<sub>PtH</sub> = 99.5 Hz, H3,4).

### Physical Measurements

NMR spectra were recorded on Bruker AC 250 (<sup>1</sup>H: 250.13 MHz, <sup>13</sup>C: 62.90 MHz) or Bruker Avance 400 spectrometers (<sup>1</sup>H: 400.13 MHz, <sup>13</sup>C: 100.3 MHz) in CDCl<sub>3</sub> at 30 °C; chemical shifts were referenced to ext. TMS. UV/VIS absorption spectra were recorded on Bruins Instruments Omega 10 and Hewlett-Packard 8453 Diode Array spectrophotometers.

### Theoretical Calculations

Ground state electronic structure calculations on model complexes [PtCl<sub>n</sub>(R)<sub>m</sub>(Me-DAB)] have been done on the base of density-functional theory (DFT) methods using the ADF2004.01 [29, 30] and Gaussian 03 [31] program packages. The lowest excited states of the closed shell complexes were calculated by the time-dependent DFT (TD-DFT) method (both ADF and G03 programs). The electrostatic solvent effect was modelled by conductor-like polarizable continuum model CPCM [32] incorporated into G03. Nuclear spin-spin coupling constants were calculated by the CPL module [33, 34] and NMR shielding tensors by the NMR module [35] within ADF2004.01.

Within the ADF program, Slater type orbital (STO) basis sets of triple-ζ quality with polarization functions were employed for geometry optimisation and TD-DFT calculations. The inner shells were represented by frozen core approximation (1s for C, N, 2p for Cl and 1s-4d for Pt were kept frozen). Core electrons were included for calculations of NMR parameters, here quadruple-ζ with four polarization functions basis was used for Pt. The following density functionals were used within ADF: the local density approximation (LDA) with VWN parametrisation of electron gas data or the functional including Becke's gradient correction [36] to the local exchange expression in conjunction with Perdew's gradient correction [37] to the LDA expression (ADF/BP). The scalar relativistic (SR) zero order regular approximation (ZORA) was used within this study.

Within Gaussian 03 Dunning's polarized valence double-ζ basis sets [38] were used for C, N, Cl and H atoms and the quasirelativistic effective core pseudopotentials and corresponding optimized set of basis functions [39] for Pt. Hybrid Becke's three parameter functional with Lee, Yang and Parr correlation functional (B3LYP) [40] was used in Gaussian calculations (G03/B3LYP).

The geometry optimisations were performed without any symmetry constrains, the approximate symmetry was used for description of

MOs and spectra. All results discussed correspond to optimized geometries.

**Crystal Structure Determination of [Pt(Me)<sub>2</sub>(iPr-DAB)], [Pt(Mes)<sub>2</sub>(iPr-DAB)] and [PtCl(Mes)(iPr-DAB)].** Suitable crystals were grown by slow evaporation of the solvent from saturated solutions of [Pt(Me)<sub>2</sub>(iPr-DAB)] in diethyl ether, [Pt(Mes)<sub>2</sub>(iPr-DAB)] in toluene, or [PtCl(Mes)(iPr-DAB)] in CH<sub>2</sub>Cl<sub>2</sub>. The X-ray data were collected at 173(2) K on a Siemens P4 diffractometer, using graphite monochromated Mo-Kα radiation (λ = 0.71073 Å) and employing Wyckoff scans. Further details are given in Table 1. All structures were solved by direct methods using the SHELXTL package, while refinement was carried out with SHELXL97 employing full-matrix least-squares methods on F<sup>2</sup> with F<sub>o</sub><sup>2</sup> ≥ 2σ(F<sub>o</sub><sup>2</sup>) [41]. All non-hydrogen atoms were refined anisotropically, hydrogen atoms were introduced using appropriate riding models. Empirical absorption correction was performed using Ψ-scans. Crystallographic data have been deposited with the Cambridge Crystallographic Data Centre, CCDC-264430 [Pt(Me)<sub>2</sub>(iPr-DAB)], -264431 [Pt(Mes)<sub>2</sub>(iPr-DAB)], and -264432 [PtCl(Mes)(iPr-DAB)]. Copies of the information may be obtained free of charge from: The Director, CCDC, 12 Union Road, Cambridge CB2 1EZ, UK (fax: (+44)1223-336-033; e-mail: [deposit@ccdc.cam.ac.uk](mailto:deposit@ccdc.cam.ac.uk); www: <http://www.ccdc.cam.ac.uk>).

**Supporting Information:** Further figures showing the packing of the molecules in the unit cell and the molecular structure of [Pt(Me)<sub>2</sub>(iPr-DAB)] are provided. Furthermore two tables comparing experimental and calculated structural data, two tables with complete <sup>1</sup>H and <sup>13</sup>C NMR data and four tables presenting G03/B3LYP calculated one-electron energies and composition of selected MOs of [PtCl(Me)(Me-DAB)], [PtCl(Mes)(Me-DAB)] and [PtCl<sub>2</sub>(Me-DAB)] and TD-DFT (G03/B3LYP/CPCM) calculated excitation energies for [PtCl<sub>2</sub>(Me-DAB)].

**Acknowledgement.** This work was carried out in the framework of the COST D14 and D35 actions. A.K. would like to thank the late Prof. D. J. Stufkens and Dr. Joris van Slageren (University of Amsterdam) for their hospitality and for fruitful discussions. We are also grateful for a loan of K<sub>2</sub>PtCl<sub>4</sub> by Johnson Matthey (JM). S.Z. also acknowledges financial support by the Grant Agency of the Academy of Sciences of the Czech Republic (grant 1ET400400413).

### References

- [1] C. E. Whittle, J. A. Weinstein, M. W. George, K. S. Schanze, *Inorg. Chem.* **2001**, *40*, 4053–4062.
- [2] K. E. Dungey, B. D. Thompson, N. A. P. Kane-Maguire, L. L. Wright, *Inorg. Chem.* **2000**, *39*, 5192–5196.
- [3] M. Hissler, W. B. Connick, D. K. Geiger, J. E. McGarrah, D. Lipa, R. J. Lachicotte, R. Eisenberg, *Inorg. Chem.* **2000**, *39*, 447–457.

- [4] M. Hissler, J. E. McGarrah, W. B. Connick, D. K. Geiger, S. D. Cummings, R. Eisenberg, *Coord. Chem. Rev.* **2000**, *208*, 115–137.
- [5] W. B. Connick, D. Geiger, R. Eisenberg, *Inorg. Chem.* **1999**, *38*, 3264–3265.
- [6] W. Paw, S. D. Cummings, M. A. Mansour, W. B. Connick, D. K. Geiger, R. Eisenberg, *Coord. Chem. Rev.* **1998**, *171*, 125–150.
- [7] V. M. Miskowski, V. H. Houlding, *Inorg. Chem.* **1989**, *28*, 1529–1533.
- [8] V. M. Miskowski, V. H. Houlding, C.-M. Che, Y. Wang, *Inorg. Chem.* **1993**, *32*, 2518–2524.
- [9] V. H. Houlding, V. M. Miskowski, *Coord. Chem. Rev.* **1991**, *111*, 145–152.
- [10] W. Lu, M. C. W. Chan, K.-K. Cheung, C.-M. Che, *Organometallics* **2001**, *20*, 2477–2486.
- [11] C.-W. Chan, L.-K. Cheng, C.-M. Che, *Coord. Chem. Rev.* **1994**, *132*, 87–97.
- [12] N. Chaudhury, R. J. Puddephatt, *J. Organomet. Chem.* **1975**, *84* (1), 105–115.
- [13] A. von Zelewsky, P. Belser, P. Hayoz, R. Dux, X. Hua, A. Suckling, H. Stoeckli-Evans, *Coord. Chem. Rev.* **1994**, *132*, 75–85.
- [14] J. Biedermann, G. Gliemann, U. Klement, K.-J. Range, M. Zabel, *Inorg. Chem.* **1990**, *29*, 1884–1888.
- [15] M. Maestri, D. Sandrini, V. Balzani, L. Chassot, P. Jolliet, A. von Zelewsky, *Chem. Phys. Lett.* **1985**, *122*, 375–379.
- [16] A. Klein, J. van Slageren, S. Zális, *Inorg. Chem.* **2002**, *41*, 5216–5225.
- [17] W. Kaim, A. Klein, S. Hasenzahl, H. Stoll, S. Zális, J. Fiedler, *Organometallics* **1998**, *17*, 237–247.
- [18] W. Kaim, A. Klein, *Organometallics* **1995**, *14*, 1176–1186.
- [19] A. Klein, J. van Slageren, S. Zális, *Eur. J. Inorg. Chem.* **2003**, 1917–1938.
- [20] H. C. Clark, L. E. Manzer, *J. Organomet. Chem.* **1973**, *59*, 411–428.
- [21] V. de Felice, P. Ganis, A. Vitagliano, G. Valle, *Inorg. Chim. Acta* **1988**, *144*, 57–61.
- [22] K. Yang, R. J. Lachicotte, R. Eisenberg, *Organometallics* **1998**, *17*, 5102–5113.
- [23] M. Fusto, F. Giordano, I. Orabona, F. Ruffo, A. Panunzi, *Organometallics* **1997**, *16*, 5981–5987.
- [24] V. G. Albano, D. Braga, V. de Felice, A. Panunzi, A. Vitagliano, *Organometallics* **1987**, *6*, 517–525.
- [25] F. R. Hartley, *The Chemistry of Platinum, Palladium*, John Wiley & Sons, New York, 1973.
- [26] T. G. Appleton, H. C. Clark, L. E. Manzer, *Coord. Chem. Rev.* **1973**, *10*, 335–422.
- [27] C. Amovilli, V. Barone, R. Cammi, E. Cancès, M. Cossi, B. Mennucci, C. Pomelli, J. Tomasi, *Adv. Quantum Chem.* **1999**, *32*, 227.
- [28] C. Eaborn, K. Kundu, A. Pidcock, *J. Chem. Soc., Dalton Trans.* **1981**, 933–938.
- [29] G. te Velde, F. M. Bickelhaupt, S. J. A. van Gisbergen, C. Fonseca Guerra, E. J. Baerends, J. G. Snijders, T. Ziegler, *J. Comput. Chem.* **2001**, *22*, 931–967.
- [30] ADF2004.01, SCM, Theoretical Chemistry, Vrije Universiteit, Amsterdam, The Netherlands, <http://www.scm.com>.
- [31] M. J. Frisch, G. W. Trucks, H. B. Schlegel, G. E. Scuseria, M. A. Robb, J. R. Cheeseman, J. A. Montgomery, T. Vreven, K. N. Kudin, J. C. Burant, J. M. Millam, S. S. Iyengar, J. Tomasi, V. Barone, B. Mennucci, M. Cossi, G. Scalmani, N. Rega, G. A. Petersson, H. Nakatsuji, M. Hada, M. Ehara, K. Toyota, R. Fukuda, J. Hasegawa, M. Ishida, T. Nakajima, Y. Honda, O. Kitao, H. Nakai, M. Klene, X. Li, J. E. Knox, H. P. Hratchian, J. B. Cross, V. Bakken, C. Adamo, J. Jaramillo, R. Gomperts, R. E. Stratmann, O. Yazyev, A. J. Austin, R. Cammi, C. Pomelli, J. W. Ochterski, P. Y. Ayala, K. Morokuma, G. A. Voth, P. Salvador, J. J. Dannenberg, V. G. Zakrzewski, S. Dapprich, A. D. Daniels, M. C. Strain, O. Farkas, D. K. Malick, A. D. Rabuck, K. Raghavachari, J. B. Foresman, J. V. Ortiz, Q. Cui, A. G. Baboul, S. Clifford, J. Cioslowski, B. B. Stefanov, G. Liu, A. Liashenko, P. Piskorz, I. Komaromi, R. L. Martin, D. J. Fox, T. Keith, M. A. Al-Laham, C. Y. Peng, A. Nanayakkara, M. Challacombe, P. M. W. Gill, B. Johnson, W. Chen, M. W. Wong, C. Gonzalez, J. A. Pople, “Gaussian 03, Revision C.02”, Gaussian, Inc., 2004.
- [32] M. Cossi, N. Rega, G. Scalmani, V. Barone, *J. Comput. Chem.* **2003**, *24*, 669–681.
- [33] J. Autschbach, T. Ziegler, *J. Chem. Phys.* **2000**, *113*, 936–947.
- [34] J. Autschbach, T. Ziegler, *J. Chem. Phys.* **2000**, *113*, 9410–9418.
- [35] G. Schreckenbach, T. Ziegler, *J. Phys. Chem.* **1995**, *99*, 606–611.
- [36] A. D. Becke, *Phys. Rev. A* **1988**, *38*, 3098–3100.
- [37] J. P. Perdew, *Phys. Rev. A* **1986**, *33*, 8822–8824.
- [38] D. E. Woon, T. H. J. Dunning, *J. Chem. Phys.* **1993**, *98*, 1358–1371.
- [39] D. Andrae, U. Haeussermann, M. Dolg, H. Stoll, H. Preuss, *Theor. Chim. Acta* **1990**, *77*, 123–128.
- [40] P. J. Stephens, F. J. Devlin, C. F. Chabalowski, M. J. Frisch, *J. Phys. Chem.* **1994**, *98*, 11623–11627.
- [41] G. M. Sheldrick, *SHELXTL-PLUS: An Integrated System for Solving, Refining and Displaying Crystal Structures from Diffraction Data*; Siemens Analytical X-Ray Instruments Inc., Ed.: Madison, W. I., 1989. G. M. Sheldrick, *SHELXL-97: A program for Crystal Structure Determination*; Universität Göttingen, Ed.: Göttingen, 1997.